Circulation: Cardiovascular Imaging

ORIGINAL ARTICLE

Myocardial Perfusion in Hypoplastic Left Heart Syndrome

Carsten Rickers, MD*; Philip Wegner, MD*; Michael Silberbach, MD; Erin Madriago, MD; Dominik Daniel Gabbert, PhD; Arash Kheradvar, MD, PhD; Inga Voges, MD; Jens Scheewe, MD; Tim Attmann, MD; Michael Jerosch-Herold, PhD†; Hans-Heiner Kramer, MD†

BACKGROUND: The status of the systemic right ventricular coronary microcirculation in hypoplastic left heart syndrome (HLHS) is largely unknown. It is presumed that the systemic right ventricle's coronary microcirculation exhibits unique pathophysiological characteristics of HLHS in Fontan circulation. The present study sought to quantify myocardial blood flow by cardiac magnetic resonance imaging and evaluate the determinants of microvascular coronary dysfunction and myocardial ischemia in HLHS.

METHODS: One hundred nineteen HLHS patients (median age, 4.80 years) and 34 healthy volunteers (median age, 5.50 years) underwent follow-up cardiac magnetic resonance imaging ≈1.8 years after total cavopulmonary connection. Right ventricle volumes and function, myocardial perfusion, diffuse fibrosis, and late gadolinium enhancement were assessed in 4 anatomic HLHS subtypes. Myocardial blood flow (MBF) was quantified at rest and during adenosine-induced hyperemia. Coronary conductance was estimated from MBF at rest and catheter-based measurements of mean aortic pressure (n=99).

RESULTS: Hyperemic MBF in the systemic ventricle was lower in HLHS compared with controls (1.89±0.57 versus 2.70±0.84 mL/g per min; $P<0.001$), while MBF at rest normalized by the rate-pressure product, was similar (1.25±0.36 versus 1.19±0.33; $P=0.446$). Independent risk factors for a reduced hyperemic MBF were an HLHS subtype with mitral stenosis and aortic atresia ($P=0.017$), late gadolinium enhancement ($P=0.042$), right ventricular diastolic dysfunction ($P=0.005$), and increasing age at total cavopulmonary connection ($P=0.022$). The coronary conductance correlated negatively with systemic blood oxygen saturation (r, −0.29; $P=0.02$). The frequency of late gadolinium enhancement increased with age at total cavopulmonary connection ($P=0.014$).

CONCLUSIONS: The coronary microcirculation of the systemic ventricle in young HLHS patients shows significant differences compared with controls. These hypothesis-generating findings on HLHS-specific risk factors for microvascular dysfunction suggest a potential benefit from early relief of frank cyanosis by total cavopulmonary connection.

Key Words: heart defects, congenital ■ hypoplastic left heart syndrome ■ Fontan circulation ■ magnetic resonance imaging ■ myocardial perfusion imaging

The 3-stage surgical palliation of hypoplastic left heart syndrome (HLHS) is considered one of the major achievements of congenital heart surgery.[1,2] The Fontan circulation after complete surgical palliation presents new challenges for understanding potential pathophysiological characteristics that increase the risk of forthcoming right ventricular (RV) failure.[1,3,4] Among those, the status of the coronary microcirculation in HLHS has been relatively

Correspondence to: Carsten Rickers, MD, German Center for Cardiovascular Research, University Heart Center, Adult With Congenital Heart Disease Unit, University Hospital Hamburg-Eppendorf, Partner Site Hamburg/Kiel/Lübeck, Martinistrasse 52, Hamburg 20246, Germany. Email c_rickers@hotmail.com
*C. Rickers and P. Wegner contributed equally.
† M Jerosch-Herold and H-H Kramer contributed equally to conception and study execution.
The Data Supplement is available at https://www.ahajournals.org/doi/suppl/10.1161/CIRCIMAGING.121.012468.
For Sources of Funding and Disclosures, see page 952.

Circulation: Cardiovascular Imaging is available at www.ahajournals.org/journal/circimaging

CLINICAL PERSPECTIVE

The status of the coronary microcirculation in the systemic right ventricles (RVs) of patients with hypoplastic left heart syndrome (HLHS) is largely unknown. Coronary dysfunction and myocardial ischemia are important factors in the etiology of heart disease with and without preserved ejection fraction. This prospective cardiac magnetic resonance study aimed at identifying the determinants and risk factors of microvascular coronary dysfunction and myocardial ischemia in HLHS. Volumes and function of the systemic ventricle, myocardial perfusion at rest, and during adenosine-induced hyperemia, diffuse myocardial fibrosis, and late gadolinium enhancement were assessed in 4 different anatomic subtypes of HLHS. Cardiac magnetic resonance imaging in 119 HLHS patients and 34 healthy controls revealed that the coronary microcirculation of the systemic ventricle in young HLHS patients is markedly impaired compared with controls. The coronary conductance at rest correlated negatively with systemic blood oxygen saturation, suggesting a form of compensatory coronary vasodilation, and the frequency of late gadolinium enhancement increased with age at total cavopulmonary connection. Diastolic dysfunction, the presence of the mitral atresia/aortic stenosis subtype, and an older age at total cavopulmonary connection appear to be risk factors for RV microcirculatory dysfunction. In summary, this study provides new insights into factors unique to HLHS patients that affect the RV microcirculation and tissue structure and may generate novel hypothesis for future long-term studies. Such studies are required to investigate the role of the RV microcirculation leading to RV dysfunction in HLHS patients over time.

Nonstandard Abbreviations and Acronyms

AA	aortic atresia
AS	aortic stenosis
CMR	cardiac magnetic resonance
HLHS	hypoplastic left heart syndrome
LGE	late gadolinium enhancement
LV	left ventricle
MA	mitral atresia
MBF	myocardial blood flow
MS	mitral stenosis
RPP	rate-pressure product
RV	right ventricle
TCPC	total cavopulmonary connection
VCC	ventriculocoronary connection

unexplored, despite the fact that the inevitable extensive vascular surgery during the Norwood operation often leads to sympathetic denervation of the heart.[5–7] Thus, the systemic RV's coronary microcirculation in children with HLHS is assumed to differ significantly compared with normal left ventricles (LVs) in non-HLHS subjects.[8–11] Moreover, myocardial perfusion may vary among HLHS anatomic subtypes, in light of previous studies that assigned a higher risk for stage 1 and interstage mortality to the subtype with mitral stenosis (MS) and aortic atresia (AA) compared with the other subtypes.[2,12,13]

Positron emission tomography with radioactive flow tracers has been considered the gold standard to quantify myocardial blood flow (MBF).[14–18] However, due to radiation exposure, nuclear medicine methods are generally less preferred in children. Over the last decade, cardiac magnetic resonance (CMR) imaging has become a major alternative for quantitative determination of myocardial perfusion at rest and during maximal hyperemia.[19]

This study aims to quantify the global and regional coronary microcirculation in the systemic RV of HLHS patients compared with control subjects with healthy hearts and on that basis identify HLHS-specific risk factors for microvascular dysfunction.

METHODS

The data that support the findings of this study are available from the corresponding author upon reasonable request.

Study Subjects

This prospective CMR cohort consists of 119 HLHS patients from the University of Schleswig-Holstein/Campus Kiel Medical Center (median age, 4.8; 67.23% women). The patients' cohort includes all 4 major anatomic subtypes of MS/aortic stenosis (AS), MS/AA, mitral atresia (MA)/AS, and MA/AA as previously described by our center (Figure 1).[20] All HLHS patients underwent a comprehensive CMR study after the final palliative step with completion of the total cavopulmonary connection (TCPC) using an intraatrial lateral tunnel. The same lead surgeon (J.S.) and his team at the University of Schleswig-Holstein/Campus Kiel Medical Center operated on all the studied HLHS patients. Patients with moderate or severe tricuspid or aortic valve insufficiency or with a hemodynamically significant gradient (>1.6 m/s by Doppler echocardiography) in the RV outflow tract or aorta, as well as patients with pacemakers were excluded from the study. Most patients (86%) were sedated with propofol and midazolam during the CMR scan. Heart rate, respiratory motion, oxygen saturation, and noninvasive blood pressure were monitored during CMR studies. The study was performed according to the ethical standards of the 1964 Declaration of Helsinki and its later amendments and was approved by our hospital's institutional review board (No. D526/16). Informed written consent was obtained from the patients or their legal guardians.

The control group was recruited among the subjects who underwent a clinically indicated CMR study with administration of gadolinium-based contrast. More specifically, 18 subjects (median age, 5.1 years; 44.4% women) who were ruled out

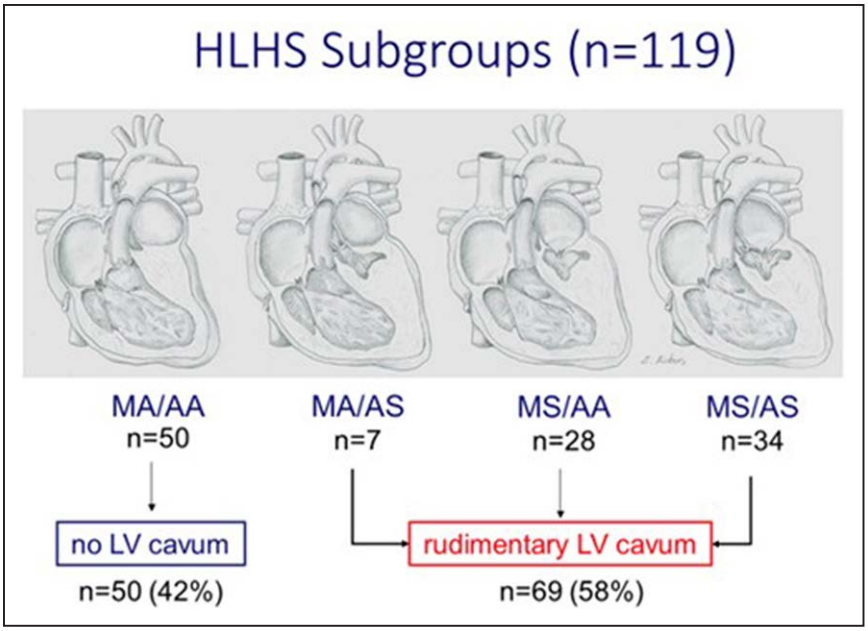

Figure 1. Distribution of hypoplastic left heart syndrome (HLHS) subtypes. A visible left ventricular (LV) cavum is present in mitral atresia (MA)/aortic stenosis (AS), mitral stenosis (MS)/aortic atresia (AA), and MS/AS (58% of cases). The MA/AA subtype does not have any visible LV cavum (42% of cases).

for any cardiac abnormality were selected as control subjects at the University of Schleswig-Holstein/Campus Kiel Medical Center. To increase the diversity of control subjects, we included the perfusion studies of an additional 16 healthy subjects (<14 years; median age, 7.1 years) from a previously published study[21] from the Oregon Health and Science University, as performed by coauthors E.M., M.S., M.J.-H., and their colleagues using the same type/model of 3T magnetic resonance scanner. All 34 control subjects from Kiel and Oregon underwent the same first-pass magnetic resonance perfusion protocol, which has been originally established by the same investigator (M.J.-H.) at both institutions.[21]

CMR Techniques

CMR studies were performed on a 3.0T MRI scanner (Achieva 3.0T; Philips Medical Systems, the Netherlands), using a phased-array coil for cardiac imaging, or for small children, a phased-array coil for extremities (SENSE Cardiac coil, SENSE Flex-L coil; Philips Medical Systems). Gradient echo cine CMR (Figure 2A) with retrospective ECG gating was performed to evaluate RV volumes, mass and systolic function, and to define the anatomic subtypes, applying the following scan parameters: field of view, ≤280×224 mm; voxel size, 1.6×1.5×5 mm^3; repetition time/echo time, 3.6/1.8 ms; 25 cardiac phases; nonbreath-hold; number of repetitions, 2; and total scan duration, 3 to 6 minutes. Myocardial perfusion images (Figure 2B) were acquired with an ECG-gated, multislice, saturation-recovery-prepared, single-shot gradient echo sequence with the following parameters: repetition time/echo time/flip angle, 1.2/2.6 ms/20°; 192×160 acquisition matrix; voxel size, ≈1.8×2.0; parallel imaging ×2 acceleration with sensitivity encoding (SENSE); slice, 10 mm; 2 slices/RR; 2 short-axis slices; and 60 dynamics. A low-dosage gadolinium contrast bolus (0.03 mmol/kg of Magnevist; Bayer, Germany) was administered through an antecubital vein with a power injector (MEDRAD Spectris, Bayer, Germany) at a rate of 4 mL/s. Maximal hyperemia was induced by intravenous adenosine with a stepwise dosage escalation from 50 µg/kg per minute, through 100 µg/kg per minute, to 140 µg/kg per minute over ≈9 minutes (3 minutes per stage), before the start of the stress perfusion scan. The adenosine infusion was turned off once the contrast bolus appeared in the LV on the reconstructed perfusion images (≈2 seconds latency time).[22] Rest perfusion images were acquired first, and hyperemic flows were measured with at least 20 minutes of delay after the rest scan.

To reach a total contrast dosage of 0.1 mmol/kg, a top off bolus was administered after the perfusion studies. Approximately 15 minutes later, late gadolinium enhancement

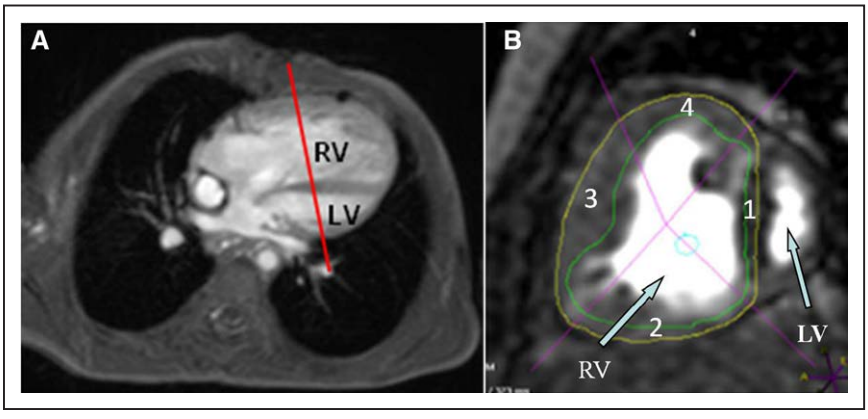

Figure 2. Cardiac magnetic resonance images of an hypoplastic left heart syndrome (HLHS) patient with subtype mitral stenosis/aortic stenosis in Fontan circulation.
A, The red line on the long-axis view (4-chamber view) from a cine acquisition denotes the orientation of short-axis image slices. **B**, For perfusion image analysis, the right ventricular (RV) wall in short-axis view was divided into 4 anatomic segments (1, septal/posterior; 2, inferior; 3, anterior; 4, superior). This is a typical first-pass perfusion image acquired during hyperemia in an HLHS patient with rudimentary left ventricular (LV) cavum.

(LGE) images were acquired with an inversion recovery–prepared 3-dimensional gradient echo sequence (field of view, 300×178×80 mm; voxel size, 1.17×1.27×10 mm; repetition time/echo time, 3.7/1.83 ms; flip angle, 15°; TI adjusted to null normal myocardium) with respiratory navigator for detection of diaphragmatic motion. The presence and location of LGE was qualitatively identified within the myocardium by windowing images to null the signal in normal myocardium. Myocardial and blood T1s were quantified with a cine Look-Locker technique in one short-axis slice in the mid-RV as described previously.[23,24]

Hemodynamic Measurements During Cardiac Catheterization

Cardiac catheterization was routinely performed under deep sedation on the day after the CMR scan. The full hemodynamic assessment included measurements of the mean aortic pressure and the RV end-diastolic pressure. Cine angiograms, including a selective injection into the native aortic root were acquired in standard projections and used to identify ventriculocoronary connections (VCCs) as previously described by our group.[25]

RV diastolic function was defined as an invasive end-diastolic pressure >10 mm Hg concordant with previous studies on diastolic dysfunction in Fontan patients.[26,27]

Image Analysis and Calculations

All CMR studies were analyzed on a workstation with dedicated software (ViewForum release 6.3; Philips Medical Systems). Anatomic HLHS subtypes were determined from axial and short-axis magnetic resonance cine image stacks and echocardiography. RV end-diastolic and end-systolic volumes were determined by planimetry of all short-axis images. Stroke volume was calculated by defining the RV volume at end diastole and then subtracting the RV volume at end systole. RV ejection fraction was calculated by dividing the stroke volume by the RV end-diastolic volume. LGE in the RV was quantified using the full-width, half-maximum criterion and expressed in grams or percentage of RV mass.

The perfusion images were segmented along the endo- and epicardial borders, and the RV myocardium was subdivided into 4 segments of equal angular extent from the RV centroid point (Figure 2B). The region of interest was drawn in the center of the RV to sample the arterial input of gadolinium contrast. This arterial input was corrected for saturation effects, using a model-based calibration. MBFs were estimated by model-independent deconvolution of the myocardial signal-intensity curves with the saturation-corrected arterial input measured, as described previously.[28] Examples of signal-intensity curves for an HLHS patient and a volunteer are shown in Figure I in the Data Supplement. Unless stated otherwise, all results for MBF at rest refer to the MBF values normalized by the patient's rate-pressure product (RPP; heart rate in beats per minute multiplied by systolic pressure in mm Hg/10^4). RPP was used here as a surrogate measure for the resting cardiac workload. In keeping with previous studies of MBF with positron emission tomography[29,30] and magnetic resonance imaging,[31] the MBF at rest was normalized by the RPP. RPP was calculated as heart rate, multiplied by systolic blood pressure and divided by 10 000, to result in MBF values around 1.0, not dissimilar to uncorrected MBF. Hyperemic MBF was not normalized by RPP, since the hyperemic response is caused by vasodilation with adenosine, which at best has a weak association with the cardiac workload. Coronary conductance was estimated from resting MBF in mL/min per gram, divided by the mean aortic pressure (mm Hg)[32] measured during catheterization within a day of the CMR study.

Look-Locker images were segmented along the RV (HLHS) or LV (controls) endo- and epicardial borders, which were further divided into 6 standard segments. T1 was determined for each segment with a nonlinear least-squares algorithm and correction for radiofrequency pulse effects. The myocardial partition coefficient for gadolinium was estimated as the rate of change of myocardial change of R1, as a function of the R1 change in the blood pool. The extracellular volume fraction for each segment was calculated as the product of the partition coefficient with (1—hematocrit fraction), as described in previous studies.[33]

Statistical Analysis

Statistical analysis was performed using the R software (version 4.0.2, 2019; R Foundation for Statistical Computing, Vienna, Austria).[34] Data are reported as mean±SD or if not normally distributed, as median and interquartile range. Means between two groups were compared with the Student *t* test or the Wilcoxon-Mann-Whitney test as nonparametric analog. Fisher exact test was used to test associations between categorical variables. ANOVA was used to compare multiple groups, and *P* values obtained with multiple post hoc testing were adjusted with the Holm method. The strength of correlations between variables was assessed with Spearman rank correlation. A multivariate linear regression model was constructed for hyperemic MBF and included anatomic subtypes, the presence of a rudimentary LV, age at the time of TCPC, presence of LGE or percentage of LGE, RV diastolic dysfunction, oxygen saturation, age at the time of CMR scan, and sex as predictors. The presence of LGE was analyzed with a multivariate logistic regression model. Predictors considered for the logistic regression model were age at TCPC, age at the time of CMR scan, HLHS subtype, and hyperemic MBF. The final set of predictors for linear and logistic regression models was determined by stepwise forward and backward selection of predictors using the Akaike Information Criterion (stepAIC function in R package MASS) to arrive in each case at the most parsimonious model. Variance inflation factors were determined to guard against any potential predictor collinearities, for example, age at TCPC and age at the time of CMR scan, using a variance inflation factor threshold of 2.5. Statistical tests were 2 tailed, and *P* values of <0.05 were considered statistically significant.

RESULTS

Patient Characteristics

HLHS patients underwent CMR at a median of 1.8 years (interquartile range, 2.7; range, 0.8–16 years) after TCPC. Six HLHS patients with tricuspid regurgitation (n=3) or aortic regurgitation (n=3) were excluded from further analysis. The HLHS patients were comparable in age,

weight, body height, and body surface area to controls, as shown in Table 1. Heart rate, systolic blood pressure, and the RPP were significantly lower in HLHS ($P<0.01$). A Blalock-Taussig shunt in the context of the Norwood operation was initially established in 115 (96.6%) HLHS patients, and 4 (3.4%) received a (nonvalved) RV-PA conduit (Sano-Shunt). Additional patient characteristics are summarized in Table 1.

The distribution of HLHS anatomic subtypes (Figure 1) was comparable to previous studies.[2,13,35] A rudimentary LV with a visible LV cavum on short-axis CMR images was present in the subtypes MA/AS (6%), MS/AA (24%), and MS/AS (29%), see example in Figure 2. In the subtypes MA/AA (42% of cases), no visible LV cavum was present.

RV Volumes and Function

Table 2 summarizes the CMR results for the systemic ventricle in controls and HLHS patients. In comparison to healthy control subjects, HLHS patients had higher indexed systemic ventricle volumes at end diastole and end systole, a higher indexed wall mass, and a lower ejection fraction but a similar cardiac index. The RV cardiac index did not vary significantly (ANOVA, $P=0.128$) among HLHS anatomy subtypes. RV volume or function parameters did not significantly differ among the HLHS subtypes. RV ejection fraction correlated negatively with age at TCPC (r, −0.244; $P=0.01$).

Late Gadolinium Enhancement

LGE imaging was available for 103 (87%) HLHS patients. LGE imaging was performed at the end of the exam and had to be skipped in patients who awoke early from sedation. LGE was not reported for cases where part of the RV wall was affected by artifacts from metallic implants. Myocardial LGE was detected in 17 (14%) of the HLHS patients. In 8 (7%) patients, LGE was present in the RV, with a median of 2.8 g (6.9 % of RV mass; interquartile range, 6.7%) of scar tissue. The age at TCPC and hyperemic MBF were identified by stepwise selection as best predictors in a logistic regression model for the presence of LGE. Based on this logistical regression model, LGE was more likely with increasing age at TCPC (odds ratio, 2.1:1 for 1-year increase; $P=0.019$; Figure II in the Data Supplement), while the probability of LGE trended lower with increasing hyperemic MBF (odds ratio, 0.32:1 for 1 mL/min per g increase of hMBF; $P=0.066$).

Myocardial Perfusion

MBF at rest was estimated in 108 (91%) and hyperemic MBF in 101 (85%) of HLHS patients. Myocardial perfusion could not be quantified in cases with severe

Table 1. Clinical Characteristics and CMR–Computed Measures in HLHS Patients and Controls

	Control (n=34)	HLHS (n=119)	*P* value
Female sex	18 (52.94)	81 (67.23)	<0.001
Age at CMR, y	5.50 (3.42–8.40)	4.80 (4.00–6.55)	0.797
Height, cm	115.27±27.73	111.57±17.56	0.472
Weight, cm	24.94±13.29	20.75±10.23	0.101
BSA, m^2	0.88±0.34	0.79±0.24	0.184
O_2 saturation, %	98.43±1.27	90.52±4.68	0.008
Hematocrit, %	41.33±1.75	42.36±3.74	0.378
Heart rate, bpm	89.15±17.78	75.94±15.93	<0.001
BP sys, mm Hg	92.00±15.89	82.96±12.19	0.005
BP dias, mm Hg	45.52±14.07	43.35±8.98	0.460
MAP, mm Hg	60.95±13.36	56.42±9.30	0.080
RPP, bpm×mm Hg/10^4	0.82±0.21	0.64±0.16	<0.001
Medication usage in HLHS patients			
β-Blocker		7 (5.8)	
Aspirin		82 (68.3)	
Diuretics		7 (5.8)	
ACE inhibitor		19 (15.8)	
Marcumar		16 (13.3)	
HLHS-specific characteristics			
HLHS anatomy subtypes			
MA/AA		50 (42.0)	
MA/AS		7 (5.9)	
MS/AA		28 (23.5)	
MS/AS		34 (28.6)	
Age at TCPC, y (median with IQR)		2.59 (2.21–2.96)	
Total bypass time, min		394±106	
Ischemia time, min		69±51	
Fenestration		90 (75.6)	
Fenestration closure			
Spontaneous		6 (5.0)	
Interventional		23 (19.3)	
Native ascending aorta			
Diameter, mm (echocardiography at birth)		3.4±1.3	
Diameter, mm/m^2 (echocardiography at birth)		16.1±6.5	
Diameter, mm (date of CMR)		8.5±3.2	
Diameter, mm/m^2 (date of CMR)		10.8±4.2	
Cardiac catheterization			
Mean aortic pressure, mm Hg		65±11	
RV-EDP mean, mm Hg		5.63±2.33	
RV-EDP max, mm Hg		8.65±2.84	
Transpulmonary gradient (SVC–AP), mm Hg		5.21±1.21	
Mean pressure lateral tunnel		12.87±2.19	

Continuous and normally distributed variables are summarized as mean±SD and otherwise as median (interquartile range). Counts are shown as number (%). *P* values are from the Wilcoxon test and Fisher exact test (sex). AA indicates aortic atresia; ACE, angiotensin-converting-enzyme; AP, atrial pressure; AS, aortic stenosis; BP dias, diastolic blood pressure; BP sys, systolic blood pressure; BSA, body surface area; CMR, cardiac magnetic resonance imaging; EDP, end-diastolic pressure; HLHS, hypoplastic left heart syndrome; IQR, interquartile range; MA, mitral atresia; MAP, mean arterial pressure; MS, mitral stenosis; RPP, rate-pressure product; RV, right ventricle; SVC, superior vena cava; and TCPC, total cavopulmonary connection.

Table 2. Comparison of CMR–Measured Indices in Patients With HLHS and Controls (LV)

CMR parameter	Control (n=34)	HLHS (n=119)	
EDV, mL/m²	53.24±13.19	75.97±18.26	<0.001
ESV, mL/m²	17.57±6.80	35.15±13.24	<0.001
Wall mass, g/m²	49.75±13.24	67.28±19.71	<0.001
ECV	0.26±0.02	0.34±0.08	0.001
Ejection fraction, %	67.62±6.40	54.37±8.83	<0.001
Cardiac index [mL/(min×m²)]	3.03±0.75	3.28±1.01	0.232
Rest MBF, mL/min per g	0.92±0.16	0.75±0.17	<0.001
Rest MBF RPP-norm, mL/min per g	1.19±0.33	1.25±0.36	0.446
Hyperemic MBF, mL/min per g	2.70±0.84	1.89±0.57	<0.001
Heart rate (hyperemia), bpm	118.31±23.71	93.46±15.38	0.001
Perfusion reserve	3.00±1.06	2.59±0.78	0.045
Perfusion reserve (rest MBF normalized by RPP)	1.95±0.85	1.63±0.53	0.165

Values for ventricular volumes and function pertain to the systemic ventricle in controls (LV) and HLHS patients (RV). *P* values are from the Wilcoxon or Fisher exact test. CMR indicates cardiac magnetic resonance; ECV, extracellular volume fraction; EDV, end-diastolic volume; ESV, end-systolic volume; HLHS, hypoplastic left heart syndrome; LV, left ventricle; MBF, myocardial blood flow; norm, normalized; RPP, rate-pressure product; and RV, right ventricle.

image artifacts due to metallic implants, foldover artifacts not apparent before contrast enhancement, or because the patient refused contrast or sedation wear off and the patient became restless. At the segmental level, MBF at rest was quantified in 86% (744 of 864) of all segments and hyperemic blood flow in 84% (680 of 808) of all segments. Segmental could not be quantified due to spillover from the blood pool around the RV outflow tract because the myocardial wall was too thin or due to the presence of image artifacts. MBF of the systemic ventricle at rest, normalized by the RPP, did not significantly differ between HLHS patients and control subjects (rest MBF, 1.25±0.36 versus 1.19±0.33 mL/min per g; *P*=0.446), but during maximal hyperemia, HLHS patients had MBFs significantly lower than controls (hyperemic MBF, 1.89±0.57 versus 2.70±0.84 mL/min per g; *P*<0.001), as shown in Figure 3. Myocardial perfusion reserve, calculated as hyperemic MBF, divided by rest MBF was also lower in HLHS patients compared with controls (2.59±0.78 versus 3.00±1.06; *P*=0.045), but once rest MBF was normalized by the RPP, the difference of the reserve was insignificant (*P*=0.165; Table 2).

Hyperemic MBF varied among anatomic subtypes (*P*=0.058 for ANOVA test) and was significantly lower by 0.33 mL/min per gram in the MS/AA group compared with the MA/AA group (adjusted *P*=0.017; Figure 4) and with respect to all other anatomic subtypes pooled together (*P*=0.019 for *t* test). VCCs, not uncommon in the MS/AA subtypes,[13,25] were found in 8 (29%) HLHS patients with the MS/AA subtype. The presence of VCCs had no significant effect on myocardial perfusion at rest or hyperemia. Late gadolinium enhancement in HLHS was associated with a reduced rest MBF (RPP normalized; *P*=0.040) and hyperemic

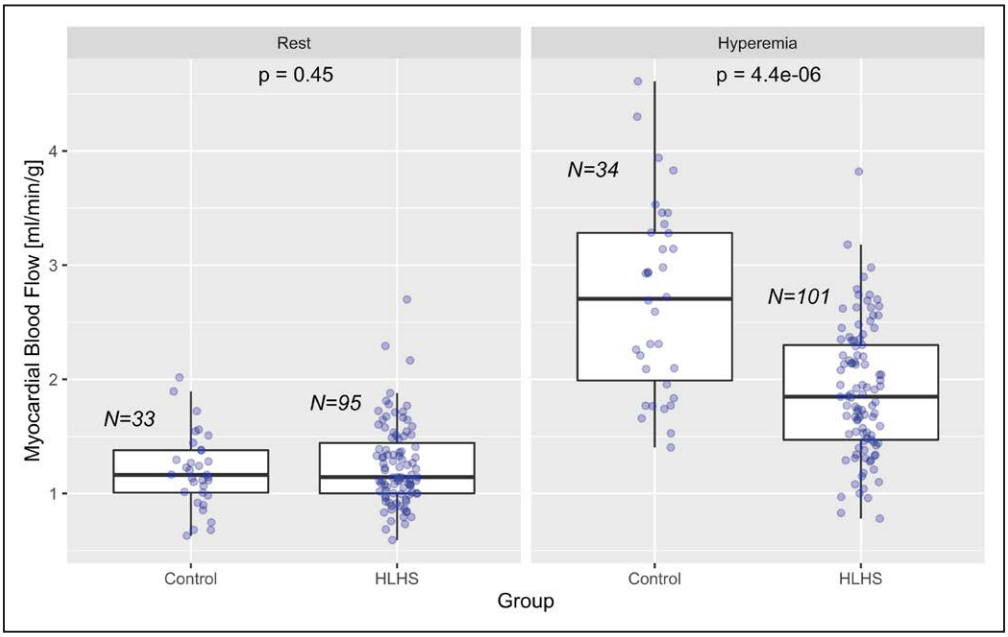

Figure 3. Myocardial blood flow in hypoplastic left heart syndrome (HLHS) and controls at rest and hyperemia. Normalized at rest myocardial blood flow did not differ between HLHS and controls (**left**), since the rate-pressure product was significantly different between the two groups (0.82±0.21 vs 0.64±0.16 bpm mm Hg/10⁴; *P*<0.001). Myocardial blood flow at rest without normalization by the rate-pressure product (not shown) was significantly lower in the hypoplastic left heart syndrome group due to the lower cardiac workload. Hyperemic myocardial blood flow was significantly lower in patients with HLHS compared with healthy controls. *P* values are from unpaired Student *t* tests.

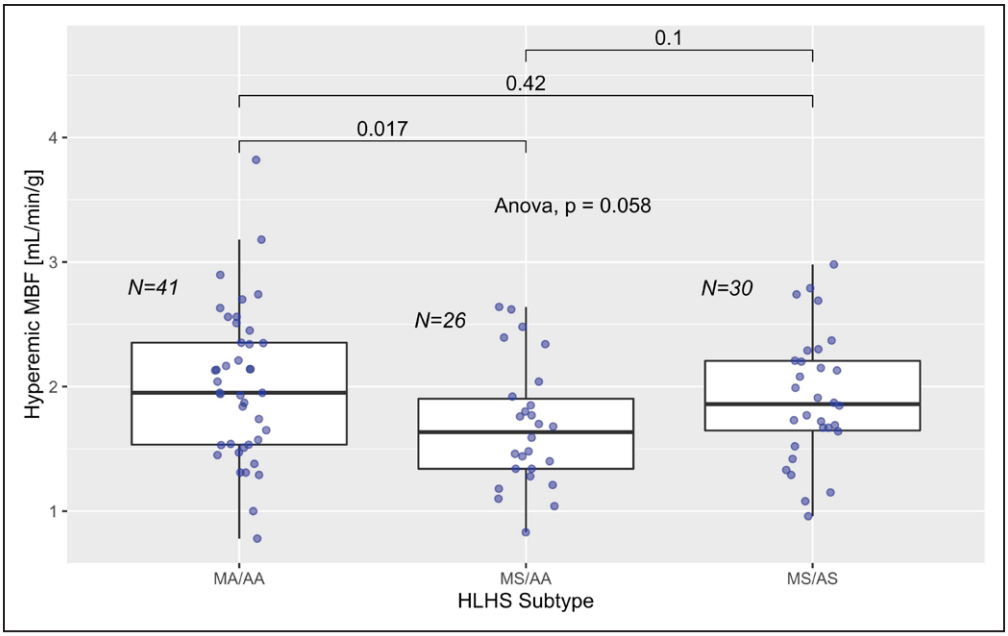

Figure 4. Hyperemic myocardial blood flow (MBF) in anatomic subtypes of hypoplastic left heart syndrome (HLHS).
Hyperemic MBF was the lowest in the anatomic subtype of HLHS with mitral stenosis (MS) and aortic atresia (AA; adjusted *P*=0.017 compared with mitral atresia [MA]/AA). *P* values are from Student *t* test and adjusted for multiple comparisons. AS indicates aortic stenosis.

MBF (*P*=0.042; Figure 5A and 5B). Hyperemic MBF was lower in the posterior wall segment when a rudimentary LV cavum was present (*P*=0.016; Figure III in the Data Supplement).

In HLHS patients, the coronary conductance at rest, calculated as rest MBF, divided by the mean aortic pressure measured during catheterization within a day of the CMR exam, averaged 0.018±0.0031 mL/min per g/mm Hg. The coronary conductance at rest was negatively associated with blood O_2 saturation (r, −0.3; *P*=0.017; Figure 6A). The blood O_2 saturation correlated negatively with the RV cardiac index (r, −0.34; *P*<0.001; Figure 6B) and was negatively associated with blood hematocrit (r, 0.22; *P*=0.017) and blood hemoglobin (r, 0.28; *P*=0.003).

Cardiac Catheterization

Invasive hemodynamic measurement results are shown in Table 1. Blood pressures (mm Hg) within the lateral tunnel, RV, and aorta were in the similar range/age previously reported for children with HLHS in Fontan circulation from our center and others.[36,37] There were no significant pressure differences among anatomic HLHS subtypes. Of the 99 patients who underwent coronary catheterization, 12

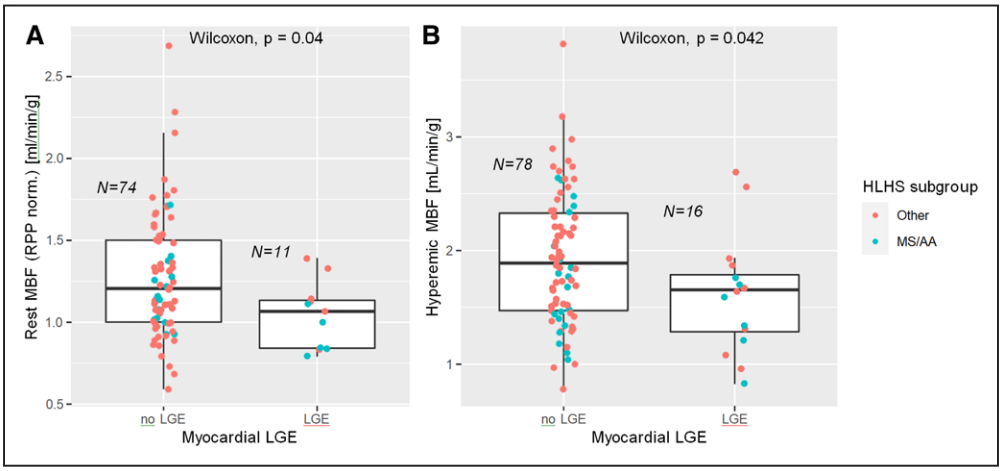

Figure 5. Myocardial blood flow (MBF) at rest and hyperemia in hypoplastic left heart syndrome (HLHS) with or without late gadolinium enhancement (LGE).
A, Myocardial LGE, which is relatively infrequent in the HLHS cohort (14%), was associated with a lower MBF at rest (*P*=0.040). **B**, LGE was also associated with a lower hyperemic MBF (*P*=0.042). AA indicates aortic atresia; MS, mitral stenosis; and RPP, rate-pressure product.

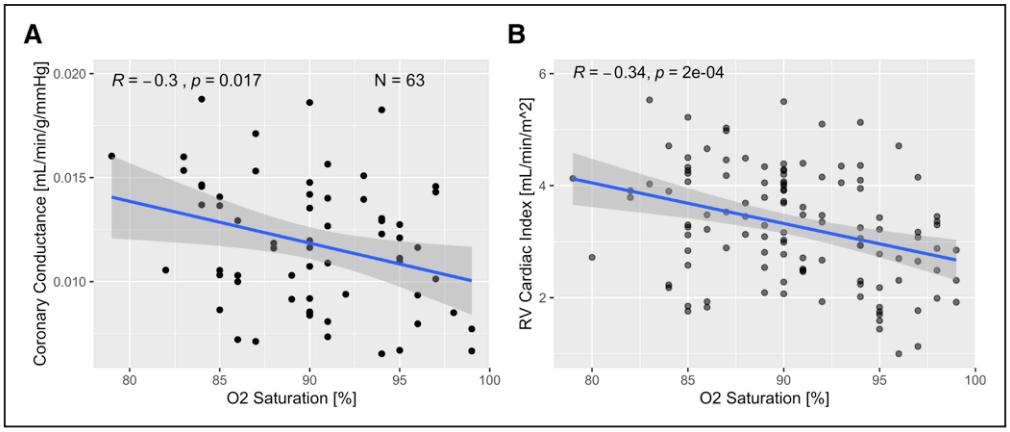

Figure 6. Association of coronary conductance and right ventricular (RV) cardiac index with blood oxygen saturation. **A**, Coronary conductance was negatively associated with blood O_2 saturation, suggesting a form of compensatory vasodilation at baseline. Coronary conductance was estimated from myocardial blood flow at rest (mL/min per g), divided by the mean aortic pressure (mm Hg) as measured during catheterization within a day of the cardiac magnetic resonance study. **B**, The RV cardiac index decreased with blood O_2 saturation (both $P<0.001$). The continuous lines in the graph were calculated with linear models for the variable on the y axis and O_2 saturation ($P=0.017$) as predictor.

(12%) had diastolic dysfunction (RV-end-diastolic pressure, >10 mm Hg). Diastolic dysfunction was present in 20% (5 of 25) of HLHS patients in the MS/AA subgroup and in 9% (7 of 74) for the other subgroups ($P=0.173$ for Fisher exact test).

Diastolic dysfunction was associated with a lower hyperemic MBF (1.54±0.38 versus 1.95±0.58 mL/min per g; t test $P=0.0053$).

Multivariate Prediction of Hyperemic MBF

After stepwise selection of predictors for multivariate regression model for the prediction of hyperemic MBF in HLHS, the MS/AA subtype (−0.329 mL/min per g; $P=0.034$), age at TCPC (−0.179 per year delay in TCPC; $P=0.022$), RV diastolic dysfunction (−0.316 mL/min per g; $P=0.088$), and male gender ($P=0.171$) remained in the final model. This selection of predictors did not change if LGE presence was replaced by the percentage of LGE in RV. Age at CMR, O_2 saturation, a rudimentary LV cavum, and myocardial LGE were eliminated. The model intercept estimate of 2.1 mL/min per gram corresponds to the hyperemic blood flow of a female HLHS patient with TCPC at 2.7 years, in the MA/AA anatomic subtype and without RV diastolic dysfunction (Figure IV in the Data Supplement).

Extracellular Volume Fraction

T1 mapping pre- and post-contrast were performed in 51 (43%) HLHS patients after a look-locker T1-mapping technique became available. In HLHS patients, the RV ejection fraction trended lower with increasing extracellular volume ($P=0.087$). There was no significant correlation of extracellular volume fraction with rest or hyperemic MBF, respectively.

DISCUSSION

This prospective study in a cohort of 119 HLHS patients in Fontan circulation is the first CMR-based investigation focusing on the pathophysiological characteristics that put the RV microcirculation at risk after 3-step surgical palliation. We found significant differences of the microcirculation of the systemic ventricle in HLHS patients compared with control subjects.

Effects of HLHS Subtypes on MBF

The MS/AA subtype represents a risk factor unique to HLHS patients,[2,13,35] starting with the Norwood procedure, during the interstage phase and beyond.[2,13,35,38] Over 2 decades ago, Sugiyama et al[39] observed in an angiographic and histopathologic study that myocardial fibrosis, calcification, and necrosis occur more frequently in HLHS patients with MS/AA anatomy, compared with other subtypes. They also reported an impaired RV posterior wall motion, concluding that the rudimentary LV (piggyback ventricle) is a functional burden to the heart. Siehr et al[13] noted that severe myocardial dysfunction, mostly due to coronary ischemia, is possibly related to VCCs and renders the MS/AA group more vulnerable to surgical palliation or cardiopulmonary bypass. Our data indicate that myocardial perfusion continues to be impaired in the MS/AA group after switch to Fontan circulation compared with the other anatomic subgroups, but we could not find a significant difference in patients with and without VCC's.

The reduction of hyperemic MBF related to RV diastolic dysfunction in HLHS patients parallels previous findings on the effects of LV diastolic dysfunction on microcirculary function in anatomically normal hearts with angiographically normal coronary arteries.[40] A rudimentary LV has been characterized as representing a

functional burden to the RV, manifested by diastolic dysfunction.[12,41] In our study, diastolic dysfunction was about twice as frequent in the MS/AA group (20%) with rudimentary LV compared with the other subgroups (9%).

LGE in HLHS

LGE presence in HLHS patients was associated with lower resting and hyperemic blood flows. Nevertheless, LGE did not make it into the most parsimonious model for hyperemic MBF after stepwise variable selection (Figure III in the Data Supplement), while age at the time of TCPC was retained in the final model. The presence of LGE was strongly associated with the age at TCPC completion, suggesting that LGE may partially result from later conversion to Fontan circulation (Figure I in the Data Supplement) and be a secondary effect of a later relief from cyanosis. Age at TCPC—the variable that is retained after stepwise selection—may capture multiple adverse effects to the heart besides LGE, for example, the RV end-diastolic volumen indexed by body surface area and RV end-systolic volumen indexed by body surface area increased significantly with age at TCPC, and RV ejection fraction decreased with age at TCPC independent of the age at the time of CMR. Therefore, the lateral tunnel may be advantageous to achieve an early relief of cyanosis. The current study did not show any significant association between a CMR marker of diffuse fibrosis (extracellular volume fraction) and myocardial perfusion. Further longitudinal and comparative studies need to ultimately clarify the effect of type and timing of TCPC on myocardial fibrosis and blood flow.

Coronary Conductance

There was a significant association between coronary conductance at rest and blood O_2 saturation (Figure 6A) in HLHS patients, suggesting a form of compensatory vasodilation at rest. More specifically, patients with lower oxygen saturation had a higher coronary conductance[32,42] estimated from the ratio of MBF at rest divided by the mean aortic pressure (Figure 6A). HLHS patients with lower oxygen saturation tended to have higher blood hematocrit and hemoglobin values, both of which may contribute to higher blood viscosity with decreasing O_2 saturation.[43,44] Maintaining RV myocardial perfusion in the presence of increased blood viscosity requires a compensatory increase of perfusion pressure and coronary conductance. As blood pressures are already lower than normal in many HLHS patients, compensatory coronary vasodilation at baseline appears to be the more likely response to the reduced O_2 saturation (Figure 6A). Lower O_2 saturations can reflect a higher right-to-left shunt (eg, through an open fenestration, suture dehiscence of the baffle, or veno-venous collaterals). This indicates that blood bypasses the lungs, which is compensated by an increase of the cardiac index and would be consistent with the observed correlation between O_2 saturation and cardiac index (Figure 6B).

There is a paucity of published studies on myocardial perfusion in children with HLHS. A study by Donnelly et al[8] in 1998 with ammonium positron emission tomography in a subgroup of 5 HLHS patients at a mean interval of 13.2 days after Norwood surgery, but none of them in Fontan circulation, is a notable exception.

Previous nuclear medicine studies in children with healthy hearts have shown that myocardial perfusion under stress increases ≈3-fold compared with resting perfusion.[16] The results in our control group approximately correspond to the MBF ranges at rest and hyperemia reported for children[21] and young adults.[14,15,28,30,45]

Possible Mechanisms for Impaired MBF in HLHS

Myocardial perfusion depends on the capillarization of the ventricular myocardium, which may be reduced in HLHS patients, according to a previous histological investigation by Salih et al.[10] An altered or impaired vasoreactivity due to inadequate cardiac (re-)innervation may be another mechanism that reduces MBF under stress in these patients and possibly also affects coronary vasomotor tone at rest. The Norwood operation involves surgical sectioning of the native aorta resulting in sympathetic denervation and potential inadequate cardiac reinnervation similar to transplanted hearts.[6,46–48] Extensive aortic surgery during arterial switch operation[14,49] or heart transplantation[6,46–48] is also known to impair the coronary vasodilator response. Cardiac efferent sympathetic signals affect MBF during a stress,[50] especially at the arteriolar level.

In HLHS patients with no rudimentary LV, no significant differences in hyperemic MBF between RV wall segments were observed. In contrast, patients with rudimentary LV had lower hyperemic MBF in the posterior segment (Figure II in the Data Supplement), which is the segment shared with the rudimentary LV, if present. A rudimentary LV may induce RV diastolic dysfunction in HLHS patients while the impaired diastolic relaxation is known to reduce the coronary vasodilator response.[12,36,40]

Limitations

Some study limitations should be considered for interpretation of the results. Unfortunately, catheter-based measurements within a day of CMR study were not feasible for all patients. The MA/AS subtype of HLHS is known to be a rare phenotype, and with only 7 patients in our cohort, we had to exclude them from the analysis that included anatomic subtypes as effect.

Techniques for myocardial T1 mapping and extracellular volume fraction quantification only became available on our scanner during the study. Since some patients had a short sedation, LGE imaging and the T1 mapping usually

performed at the end of the CMR protocol were not carried out in all cases. Therefore, only a subgroup of HLHS patients underwent T1 mapping (43%) or LGE imaging (87%).

Conclusions

This study investigating a cohort of 119 HLHS patients in Fontan circulation is, to the best of our knowledge, the first CMR-based investigation focusing on the pathophysiological characteristics that predispose RV microcirculation to dysfunction after 3-step surgical palliation. Compared with control subjects, CMR-based quantification of MBF in the HLHS patients' systemic ventricle revealed a significant impairment of the coronary autoregulation after complete surgical palliation. Diastolic dysfunction, the presence of the MA/AS subtype, and an older age at TCPC appear to be risk factors for RV microcirculatory dysfunction. Accordingly, the associations reported in the present article can be viewed as correlations that elucidate how known pathological features of HLHS are related to microvascular dysfunction. Microvascular dysfunction is an important factor in heart failure with reduced ejection fraction, and there is also growing evidence of its role in the etiology of heart failure with preserved ejection fraction.[51,52]

In summary, this study provides new insights into factors unique to HLHS patients that affect the RV microcirculation and tissue structure and may generate novel hypothesis for future long-term studies. Such studies are required to investigate the role of the RV microcirculation leading to RV dysfunction in HLHS patients over time.

ARTICLE INFORMATION

Received January 18, 2021; accepted September 8, 2021.

Affiliations

University Heart Center, Adult Congenital Heart Disease Unit, University Hospital Hamburg-Eppendorf, Hamburg, Germany (C.R.). Department of Congenital Heart Disease and Pediatric Cardiology (P.W., D.D.G., I.V., H.-H.K.) and Department of Cardiovascular Surgery (J.S., T.A.), University Hospital Schleswig-Holstein, Kiel, Germany. Department of Pediatric Cardiology, Doernbecher Children's Hospital, Oregon Health and Science University, Portland (M.S., E.M.). Edwards Lifesciences Center for Advanced Cardiovascular Technology, University of California Irvine (A.K.). Department of Radiology, Brigham and Women's Hospital, Harvard Medical School, Boston, MA (M.J.-H.).

Acknowledgments

We thank Traudel Hansen (CMR technologist) for her assistance in patient management. Drs Jerosch-Herold and Kramer contributed equally to conception and study execution.

Sources of Funding

This work is supported by a research grant to Dr Rickers from the Fördergemeinschaft Deutsche Kinderherzzentren e.V. (No. W-KI005; www.kinderherzen.de) and, in part, by a research grant to Dr Gabbert from the German Heart Research Foundation (No. F/27/16). Dr Kheradvar was supported by an award from the Alexander von Humboldt Foundation. Dr Silberbach was supported by the Medical Research Foundation of Oregon.

Disclosures

None.

REFERENCES

1. d'Udekem Y, Iyengar AJ, Galati JC, Forsdick V, Weintraub RG, Wheaton GR, Bullock A, Justo RN, Grigg LE, Sholler GF, et al. Redefining expectations of long-term survival after the Fontan procedure: twenty-five years of follow-up from the entire population of Australia and New Zealand. *Circulation*. 2014;130(11 suppl 1):S32–S38. doi: 10.1161/CIRCULATIONAHA.113.007764
2. Furck AK, Uebing A, Hansen JH, Scheewe J, Jung O, Fischer G, Rickers C, Holland-Letz T, Kramer HH. Outcome of the Norwood operation in patients with hypoplastic left heart syndrome: a 12-year single-center survey. *J Thorac Cardiovasc Surg*. 2010;139:359–365. doi: 10.1016/j.jtcvs.2009.07.063
3. Friedberg MK, Reddy S. Right ventricular failure in congenital heart disease. *Curr Opin Pediatr*. 2019;31:604–610. doi: 10.1097/MOP.0000000000000804
4. Khairy P, Fernandes SM, Mayer JE Jr, Triedman JK, Walsh EP, Lock JE, Landzberg MJ. Long-term survival, modes of death, and predictors of mortality in patients with Fontan surgery. *Circulation*. 2008;117:85–92. doi: 10.1161/CIRCULATIONAHA.107.738559
5. Davos CH, Francis DP, Leenarts MF, Yap SC, Li W, Davlouros PA, Wensel R, Coats AJ, Piepoli M, Sreeram N, et al. Global impairment of cardiac autonomic nervous activity late after the Fontan operation. *Circulation*. 2003;9(108 suppl 1):II180-II185. doi: 10.1161/01.cir.0000087946.47069.cb
6. Bengel FM, Ueberfuhr P, Hesse T, Schiepel N, Ziegler SI, Scholz S, Nekolla SG, Reichart B, Schwaiger M. Clinical determinants of ventricular sympathetic reinnervation after orthotopic heart transplantation. *Circulation*. 2002;106:831–835. doi: 10.1161/01.cir.0000025631.68522.9d
7. Norwood WI, Lang P, Hansen DD. Physiologic repair of aortic atresia-hypoplastic left heart syndrome. *N Engl J Med*. 1983;308:23–26. doi: 10.1056/NEJM198301063080106
8. Donnelly JP, Raffel DM, Shulkin BL, Corbett JR, Bove EL, Mosca RS, Kulik TJ. Resting coronary flow and coronary flow reserve in human infants after repair or palliation of congenital heart defects as measured by positron emission tomography. *J Thorac Cardiovasc Surg*. 1998;115:103–110. doi: 10.1016/s0022-5223(98)70448-9
9. O'Connor WN, Cash JB, Cottrill CM, Johnson GL, Noonan JA. Ventriculocoronary connections in hypoplastic left hearts: an autopsy microscopic study. *Circulation*. 1982;66:1078–1086. doi: 10.1161/01.cir.66.5.1078
10. Salih C, Sheppard MN, Ho SY. Morphometry of coronary capillaries in hypoplastic left heart syndrome. *Ann Thorac Surg*. 2004;77:903–907. doi: 10.1016/j.athoracsur.2003.07.046
11. Sauer U, Gittenberger-de Groot AC, Geishauser M, Babic R, Bühlmeyer K. Coronary arteries in the hypoplastic left heart syndrome. Histopathologic and histometrical studies and implications for surgery. *Circulation*. 1989;80(3 pt 1):I168–I176.
12. Schlangen J, Fischer G, Steendijk P, Petko C, Scheewe J, Hart C, Hansen JH, Ahrend F, Rickers C, Kramer HH, et al. Does left ventricular size impact on intrinsic right ventricular function in hypoplastic left heart syndrome? *Int J Cardiol*. 2013;167:1305–1310. doi: 10.1016/j.ijcard.2012.03.183
13. Siehr SL, Maeda K, Connolly AA, Tacy TA, Reddy VM, Hanley FL, Perry SB, Wright GE. Mitral stenosis and aortic atresia–a risk factor for mortality after the modified norwood operation in hypoplastic left heart syndrome. *Ann Thorac Surg*. 2016;101:162–167. doi: 10.1016/j.athoracsur.2015.09.056
14. Bengel FM, Hauser M, Duvernoy CS, Kuehn A, Ziegler SI, Stollfuss JC, Beckmann M, Sauer U, Muzik O, Schwaiger M, et al. Myocardial blood flow and coronary flow reserve late after anatomical correction of transposition of the great arteries. *J Am Coll Cardiol*. 1998;32:1955–1961. doi: 10.1016/s0735-1097(98)00479-3
15. Hauser M, Bengel FM, Kühn A, Sauer U, Zylla S, Braun SL, Nekolla SG, Oberhoffer R, Lange R, Schwaiger M, et al. Myocardial blood flow and flow reserve after coronary reimplantation in patients after arterial switch and ross operation. *Circulation*. 2001;103:1875–1880. doi: 10.1161/01.cir.103.14.1875
16. Hernandez-Pampaloni M, Allada V, Fishbein MC, Schelbert HR. Myocardial perfusion and viability by positron emission tomography in infants and children with coronary abnormalities: correlation with echocardiography, coronary angiography, and histopathology. *J Am Coll Cardiol*. 2003;41:618–626. doi: 10.1016/s0735-1097(02)02867-x
17. Vogel M, Smallhorn JF, Gilday D, Benson LN, Ash J, Williams WG, Freedom RM. Assessment of myocardial perfusion in patients after the arterial switch operation. *J Nucl Med*. 1991;32:237–241.
18. Yates RW, Marsden PK, Badawi RD, Cronin BF, Anderson DR, Tynan MJ, Maisey MN, Baker EJ. Evaluation of myocardial perfusion using positron emission tomography in infants following a neonatal arterial switch operation. *Pediatr Cardiol*. 2000;21:111–118. doi: 10.1007/s002469910015

19. Prakash A, Powell AJ, Krishnamurthy R, Geva T. Magnetic resonance imaging evaluation of myocardial perfusion and viability in congenital and acquired pediatric heart disease. *Am J Cardiol*. 2004;93:657–661. doi: 10.1016/j.amjcard.2003.11.045
20. Petko C, Voges I, Schlangen J, Scheewe J, Kramer HH, Uebing AS. Comparison of right ventricular deformation and dyssynchrony in patients with different subtypes of hypoplastic left heart syndrome after Fontan surgery using two-dimensional speckle tracking. *Cardiol Young*. 2011;21:677–683. doi: 10.1017/S1047951111000631
21. Madriago E, Wells R, Sahn DJ, Diggs BS, Langley SM, Woodward DJ, Jerosch-Herold M, Silberbach M. Abnormal myocardial blood flow in children with mild/moderate aortic stenosis. *Cardiol Young*. 2015;25:1358–1366. doi: 10.1017/S1047951114002583
22. Jerosch-Herold M, Muehling O, Wilke N. MRI of myocardial perfusion. *Semin Ultrasound CT MR*. 2006;27:2–10. doi: 10.1053/j.sult.2005.10.001
23. Look D, Locker D. Time saving in measurment of NMR and EPR relaxation times. *Rev Sci Instrum*. 1976;41:250–251.
24. Neilan TG, Coelho-Filho OR, Shah RV, Abbasi SA, Heydari B, Watanabe E, Chen Y, Mandry D, Pierre-Mongeon F, Blankstein R, et al. Myocardial extracellular volume fraction from T1 measurements in healthy volunteers and mice: relationship to aging and cardiac dimensions. *JACC Cardiovasc Imaging*. 2013;6:672–683. doi: 10.1016/j.jcmg.2012.09.020
25. Hansen JH, Uebing A, Scheewe J, Kramer HH, Fischer G. Angiographic evaluation of the coronary artery anatomy in patients with hypoplastic left heart syndrome. *Eur J Cardiothorac Surg*. 2012;41:561–568. doi: 10.1093/ejcts/ezr123
26. Averin K, Hirsch R, Seckeler MD, Whiteside W, Beekman RH 3rd, Goldstein BH. Diagnosis of occult diastolic dysfunction late after the Fontan procedure using a rapid volume expansion technique. *Heart*. 2016;102:1109–1114. doi: 10.1136/heartjnl-2015-309042
27. Menon SC, Gray R, Tani LY. Evaluation of ventricular filling pressures and ventricular function by Doppler echocardiography in patients with functional single ventricle: correlation with simultaneous cardiac catheterization. *J Am Soc Echocardiogr*. 2011;24:1220–1225. doi: 10.1016/j.echo.2011.08.011
28. Muehling OM, Jerosch-Herold M, Panse P, Zenovich A, Wilson BV, Wilson RF, Wilke N. Regional heterogeneity of myocardial perfusion in healthy human myocardium: assessment with magnetic resonance perfusion imaging. *J Cardiovasc Magn Reson*. 2004;6:499–507. doi: 10.1081/jcmr-120030570
29. Czernin J, Müller P, Chan S, Brunken RC, Porenta G, Krivokapich J, Chen K, Chan A, Phelps ME, Schelbert HR. Influence of age and hemodynamics on myocardial blood flow and flow reserve. *Circulation*. 1993;88:62–69. doi: 10.1161/01.cir.88.1.62
30. Muzik O, Paridon SM, Singh TP, Morrow WR, Dayanikli F, Di Carli MF. Quantification of myocardial blood flow and flow reserve in children with a history of Kawasaki disease and normal coronary arteries using positron emission tomography. *J Am Coll Cardiol*. 1996;28:757–762. doi: 10.1016/0735-1097(96)00199-4
31. Borlotti A, Jerosch-Herold M, Liu D, Viliani D, Bracco A, Alkhalil M, De Maria GL, Channon KM, Banning AP, Choudhury RP, et al; OxAMI Study Investigators. Acute microvascular impairment post-reperfused STEMI is reversible and has additional clinical predictive value: a CMR OxAMI study. *JACC Cardiovasc Imaging*. 2019;12:1783–1793. doi: 10.1016/j.jcmg.2018.10.028
32. Di Carli MF, Afonso L, Campisi R, Ramappa P, Bianco-Batlles D, Grunberger G, Schelbert HR. Coronary vascular dysfunction in premenopausal women with diabetes mellitus. *Am Heart J*. 2002;144:711–718.
33. Broberg CS, Chugh SS, Conklin C, Sahn DJ, Jerosch-Herold M. Quantification of diffuse myocardial fibrosis and its association with myocardial dysfunction in congenital heart disease. *Circ Cardiovasc Imaging*. 2010;3:727–734. doi: 10.1161/CIRCIMAGING.108.842096
34. R-Core-Team. R: A language and environment for statistical computing. R foundation for statistical computing, Vienna, Austria. Accessed April 26, 2019. http://www.R-project.Org
35. Jonas RA, Hansen DD, Cook N, Wessel D. Anatomic subtype and survival after reconstructive operation for hypoplastic left heart syndrome. *J Thorac Cardiovasc Surg*. 1994;107:1121–1127.
36. Logoteta J, Ruppel C, Hansen JH, Fischer G, Becker K, Kramer HH, Uebing A. Ventricular function and ventriculo-arterial coupling after palliation of hypoplastic left heart syndrome: a comparative study with Fontan patients with LV morphology. *Int J Cardiol*. 2017;227:691–697. doi: 10.1016/j.ijcard.2016.10.076
37. Schlangen J, Fischer G, Petko C, Hansen JH, Voges I, Rickers C, Kramer HH, Uebing A. Arterial elastance and its impact on intrinsic right ventricular function in palliated hypoplastic left heart syndrome. *Int J Cardiol*. 2013;168:5385–5389. doi: 10.1016/j.ijcard.2013.08.052
38. Glatz JA, Fedderly RT, Ghanayem NS, Tweddell JS. Impact of mitral stenosis and aortic atresia on survival in hypoplastic left heart syndrome. *Ann Thorac Surg*. 2008;85:2057–2062. doi: 10.1016/j.athoracsur.2008.02.026
39. Sugiyama H, Yutani C, Iida K, Arakaki Y, Yamada O, Kamiya T. The relation between right ventricular function and left ventricular morphology in hypoplastic left heart syndrome: angiographic and pathological studies. *Pediatr Cardiol*. 1999;20:422–427. doi: 10.1007/s002469900504
40. Rajappan K, Rimoldi OE, Dutka DP, Ariff B, Pennell DJ, Sheridan DJ, Camici PG. Mechanisms of coronary microcirculatory dysfunction in patients with aortic stenosis and angiographically normal coronary arteries. *Circulation*. 2002;105:470–476. doi: 10.1161/hc0402.102931
41. Walsh MA, McCrindle BW, Dipchand A, Manlhiot C, Hickey E, Caldarone CA, Van Arsdell GS, Schwartz SM. Left ventricular morphology influences mortality after the Norwood operation. *Heart*. 2009;95:1238–1244. doi: 10.1136/hrt.2008.156612
42. Duncker DJ, Bache RJ. Regulation of coronary blood flow during exercise. *Physiol Rev*. 2008;88:1009–1086. doi: 10.1152/physrev.00045.2006
43. Most AS, Ruocco NA Jr, Gewirtz H. Effect of a reduction in blood viscosity on maximal myocardial oxygen delivery distal to a moderate coronary stenosis. *Circulation*. 1986;74:1085–1092. doi: 10.1161/01.cir.74.5.1085
44. Rim SJ, Leong-Poi H, Lindner JR, Wei K, Fisher NG, Kaul S. Decrease in coronary blood flow reserve during hyperlipidemia is secondary to an increase in blood viscosity. *Circulation*. 2001;104:2704–2709. doi: 10.1161/hc4701.099580
45. Hauser M, Bengel FM, Hager A, Kuehn A, Nekolla SG, Kaemmerer H, Schwaiger M, Hess J. Impaired myocardial blood flow and coronary flow reserve of the anatomical right systemic ventricle in patients with congenitally corrected transposition of the great arteries. *Heart*. 2003;89:1231–1235. doi: 10.1136/heart.89.10.1231
46. Bengel FM, Ueberfuhr P, Schiepel N, Nekolla SG, Reichart B, Schwaiger M. Myocardial efficiency and sympathetic reinnervation after orthotopic heart transplantation: a noninvasive study with positron emission tomography. *Circulation*. 2001;103:1881–1886. doi: 10.1161/01.cir.103.14.1881
47. Bengel FM, Ueberfuhr P, Schiepel N, Nekolla SG, Reichart B, Schwaiger M. Effect of sympathetic reinnervation on cardiac performance after heart transplantation. *N Engl J Med*. 2001;345:731–738. doi: 10.1056/NEJMoa010519
48. Uberfuhr P, Ziegler S, Schwaiblmair M, Reichart B, Schwaiger M. Incomplete sympathic reinnervation of the orthotopically transplanted human heart: observation up to 13 years after heart transplantation. *Eur J Cardiothorac Surg*. 2000;17:161–168. doi: 10.1016/s1010-7940(99)00367-x
49. Kuehn A, Vogt M, Schwaiger M, Ewert P, Hauser M. Ventricular sympathetic innervation in patients with transposition of the great arteries after arterial switch operation and Rastelli procedure: impact of arterial dissection and coronary reimplantation. *Circ J*. 2014;78:1717–1722. doi: 10.1253/circj.cj-13-1594
50. Di Carli MF, Tobes MC, Mangner T, Levine AB, Muzik O, Chakroborty P, Levine TB. Effects of cardiac sympathetic innervation on coronary blood flow. *N Engl J Med*. 1997;336:1208–1215. doi: 10.1056/NEJM199704243361703
51. Giamouzis G, Schelbert EB, Butler J. Growing evidence linking microvascular dysfunction with heart failure with preserved ejection fraction. *J Am Heart Assoc*. 2016;5:e003259. doi: 10.1161/JAHA.116.003259
52. Taqueti VR, Solomon SD, Shah AM, Desai AS, Groarke JD, Osborne MT, Hainer J, Bibbo CF, Dorbala S, Blankstein R, et al. Coronary microvascular dysfunction and future risk of heart failure with preserved ejection fraction. *Eur Heart J*. 2018;39:840–849. doi: 10.1093/eurheartj/ehx721